MAGNETOHYDRODYNAMICS Vol. 47 (2011), No. 3, pp. 273–282

# OPTIMIZATION OF A LORENTZ FORCE FLOWMETER BY USING NUMERICAL MODELING

*C. Stelian*[1,3], *A. Alferenok*[2], *U. Lüdtke*[2], *Yu. Kolesnikov*[3], *A. Thess*[3]

[1] *Department of Physics, West University of Timisoara, Bd. V. Parvan, No.4, 300223 Timisoara, Romania*
[2] *Faculty of Electrical Engineering and Information Technology, Ilmenau University of Technology, PO Box 100565, 98684 Ilmenau, Germany*
[3] *Institute of Thermodynamics and Fluid Mechanics, Ilmenau University of Technology, PO Box 100565, 98684 Ilmenau, Germany*

Lorentz force velocimetry is based on exposing an electrically conducting fluid to a magnetic field and measuring the force acting on the magnet system. In the present work, numerical modeling is used to optimize the magnet system geometry. Numerical computations are performed for a simplified problem, where the fluid flow in a channel is approximated by a solid body moving at a constant velocity through the magnetic field. The numerical optimization is based on the analysis of the channel shape and magnet system geometry influence on the flowmeter efficiency. Computations show an increasing efficiency when the channel has a rectangular cross-section and the distance between magnets is reduced. From numerical optimization it is found that a magnet system without a yoke, weighting few kilograms, can be used for efficient flow measurements in practical applications.

**Introduction.** Lorentz force velocimetry is a contactless method for measuring the flow rate in electrically conducting melts [1–5]. Among other invasive methods of flow measurements [1, 6], Lorentz flow velocimetry has some advantages, being entirely contactless and, therefore, suitable for high temperature applications, like aluminum and steel casting.

The sketch of a transverse Lorentz force flowmeter (LFF) is shown in Fig. 1. The magnetic field produced by two permanent magnets is designed in such a way as to be predominantly transverse to the flow direction. The movement of the conducting fluid with a velocity $\mathbf{v}$ in this magnetic field $\mathbf{B}$ induces electrical currents of density $\mathbf{j}$, which interact with the magnetic field giving rise to a Lorentz force $\mathbf{F}$, acting in the opposite direction of the flow. The volume density of this force can be estimated as

$$f \sim \sigma v B^2, \tag{1}$$

where $\sigma$ is the electrical conductivity of the liquid.

The induced electrical currents generate a secondary magnetic field $\mathbf{b}$, which interacts with the primary magnetic field $\mathbf{B}$ giving rise to an opposite force $-\mathbf{F}$, acting upon the magnet system. This force has the same magnitude as the Lorentz force and acts in the opposite direction (see Fig. 1). The measurement of this force is the key idea of Lorentz force velocimetry.

The Lorentz force is proportional to the mean flow velocity when the Reynolds magnetic number $\mathrm{Rm} = \mu_0 \sigma v l$ has values less than unity ($l$ is the typical length of the flow). For most industrial flows involving liquid metals, Rm is usually less than unity. For example, in aluminum casting, the mean velocities are less than

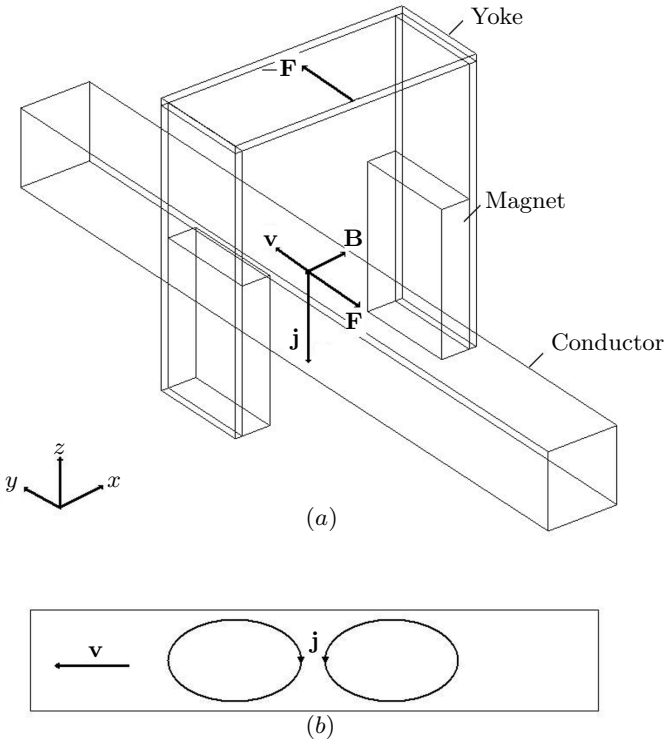


*Fig. 1.* (*a*) Sketch of a transverse Lorentz force flowmeter with two permanent magnets and a yoke; (*b*) eddy currents plotted in the $(y, z)$-plane.

1 m/s, the electrical conductivity $\sigma$ is about $\sigma = 3 \cdot 10^6\,\Omega^{-1}\mathrm{m}^{-1}$, the characterisitc flow length is 0.1 m, and $\mathrm{Rm} < 0.4$. For other liquid metals and their alloys, due to their lower conductivity, Rm becomes several times smaller.

The force acting on the magnet system depends on both the magnetic field and the velocity distribution in the fluid. From this reason, it is in general difficult to find an analytical expression for the Lorentz force related to the mean velocity of the flow. The integrated force over the volume of the flowing liquid in the channel is given by

$$F = \sigma C_v v, \tag{2}$$

where $C_v$ is the calibration coefficient related to the flow rate. The Lorentz force can be also expressed in terms of the volumetric flow rate $q$ as

$$F = \sigma C q, \tag{3}$$

where $q = Sv$ and $S$ denote the cross-section area of the liquid in the channel.

The calibration coefficient replaces the inhomogeneous magnetic field in Eq. (1) and depends on the geometry of the magnet system and flow channel. The use of LFF for industrial applications requires the calibration of this device by measuring or computing the calibration coefficient. The objective of this work is to use numerical modeling for optimization of the LFF geometry in order to increase the efficiency of Lorentz force measurements by using low-weight magnet systems.

**1. Model description.** The AC/DC Module 3.5a developed by the COMSOL Multiphysics finite element software was used for numerical modeling. The simulation was performed for a simplified case, which approximated the fluid flow

in a channel by the movement of an infinitely long conductor at a mean velocity of the flow. This approximation is based on experimental observations [1] and theoretical analysis [2] showing that the Lorentz force is weakly affected by the velocity profile for turbulent flows at high Reynolds numbers $\mathrm{Re} = 10^5 - 10^6$, which are the typical values for metallurgy.

The simulation domain contains a magnet system, a conductor considered infinitely long and a surrounding air domain with dimensions five times larger than the characteristic dimension of the magnet system. The equations solved in the magnetostatic application mode of the AC/DC module are the Ampère's law and the equation of continuity

$$\operatorname{rot} \mathbf{H} = \mathbf{j} = \sigma(\mathbf{E} + \mathbf{v} \times \mathbf{B}), \tag{4}$$

$$\operatorname{div} \mathbf{j} = 0. \tag{5}$$

where $\mathbf{H}$ is the magnetic field intensity and $\mathbf{E}$ is the electric field intensity. The problem is formulated in terms of the electric scalar potential $V$ and the magnetic vector potential $\mathbf{A}$, which are given by

$$\mathbf{B} = \operatorname{rot} \mathbf{A}, \tag{6}$$

$$\mathbf{E} = -\operatorname{grad} V - \frac{\partial \mathbf{A}}{\partial t}, \tag{7}$$

where $\partial \mathbf{A}/\partial t = 0$ in the static analysis.

Using the constitutive relation

$$\mathbf{B} = \mu_0(\mathbf{H} + \mathbf{M}), \tag{8}$$

where the magnetization vector $\mathbf{M}$ is the volume density of the magnetic dipole moments, Eqs. (4),(5) can be rewritten as

$$\nabla \times (\mu_0^{-1} \nabla \times \mathbf{A} - \mathbf{M}) - \sigma \mathbf{v} \times (\nabla \times \mathbf{A}) + \sigma \nabla V = 0, \tag{9}$$

$$-\nabla(-\sigma \mathbf{v} \times (\nabla \times \mathbf{A}) + \sigma \nabla V) = 0. \tag{10}$$

The term $-\sigma \mathbf{v} \times (\nabla \times \mathbf{A})$ stands for the density of the currents induced by the conductor movement in a static magnetic field.

Upon solution the coupled equations (9)–(10), the Lorentz force, acting on the conductor, is given by integrating the Lorentz force density over the conductor volume:

$$\mathbf{F} = \int (\mathbf{j} \times \mathbf{B}) \, \mathrm{d}V. \tag{11}$$

The magnetic insulation boundary condition, setting the tangential component of the magnetic potential to zero, is applied to the air domain boundaries

$$\mathbf{n} \times \mathbf{A} = 0. \tag{12}$$

At the interfaces between the conductor and the surrounding air domain, the continuity boundary condition is

$$\mathbf{n}(\mathbf{j}_1 - \mathbf{j}_2) = 0, \tag{13}$$

where $\mathbf{n}$ is the outward normal from the air domain. This condition sets the outward component of the electric current in the conductor to zero, when a small electric conductivity ($\sigma = 0.001\,\Omega^{-1}m^{-1}$) is attributed to the confining air region.

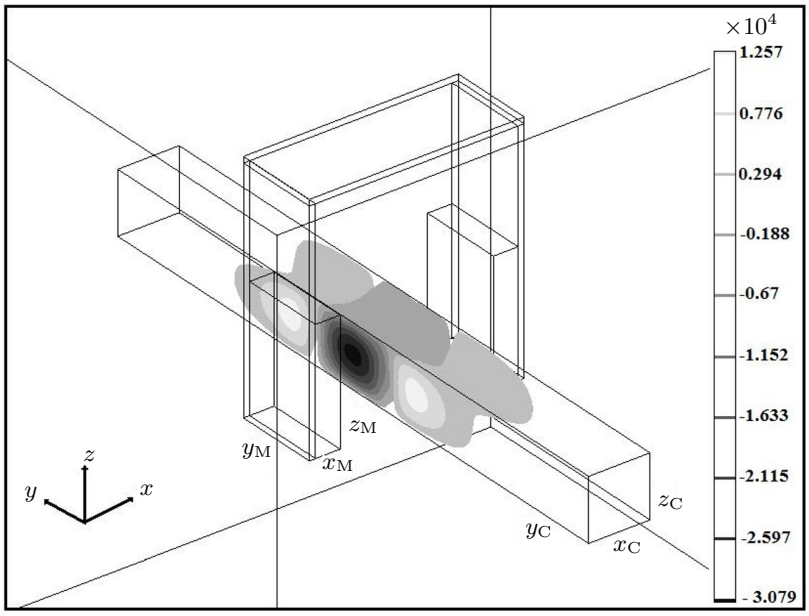


*Fig. 2.* Dry calibration configuration. Eddy currents are plotted in the aluminum bar. The component $j_z$ of the electrical current density plotted in the figure is negative in the conducting zone between the magnets and positive in the region outside the magnet system, where $B_x$ vanishes.

**2. Results and discussion.**

*2.1. Validation of the numerical model.* The numerical model is validated by comparing numerical results to Lorentz force measurements performed in [7–9]. In those experiments, the LFF calibration was performed by replacing the liquid flow in the channel by a solid aluminum bar, which is moving across the magnet system. The geometry of the experimental set-up used for the simulation is shown in Fig. 2. The aluminum bar has the length $L = 1\,\mathrm{m}$ and a rectangular cross-section. Some series of experiments were performed for various cross-sections of the aluminum bar, which were pulled through the magnetic field at different rates. The width of the reference bar was kept constant ($l = 0.1\,\mathrm{m}$) and the height ($h$) was varied from 0.025 m to 0.1 m.

The magnet system consists of two NdFeB magnets having dimensions $4\,\mathrm{cm}\times14\,\mathrm{cm}\times20\,\mathrm{cm}$ mounted on a steel yoke of 1 cm in width. The distance between the magnets is $d = 25\,\mathrm{cm}$. The conductor is positioned at a 3 cm distance above the magnets' bottom surface. The distance between the upper part of the yoke and the top surface of the magnets is $d_{\mathrm{Y-M}} = 25\,\mathrm{cm}$. The magnetic field spatial distribution in the region between the magnets was measured by a Teslameter with a transverse Hall-probe [7].

Validation is performed by comparing the measurements of the magnetic field and Lorentz force to the numerical computations. In Fig. 3*a–c*, the measured magnetic induction component $B_x$ in the $x$, $y$ and $z$ directions is compared to the numerical results, showing a good agreement. The numerical computations are performed by accounting the magnetization curve of the steel yoke. Because the magnetization of NdFeB magnets is in a wide range $M \in (860-995\,\mathrm{kA/m})$, the value used for simulation ($M_x = 970\,\mathrm{kA/m}$) was obtained by fitting the numerical

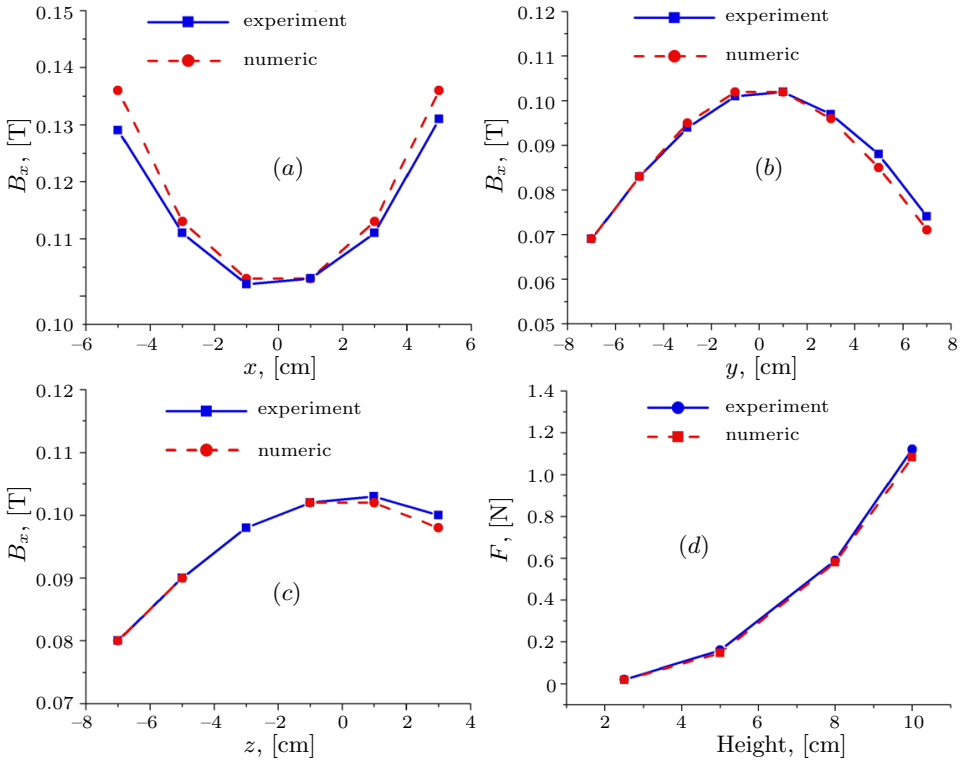


*Fig. 3.* Comparison of experimental measurements [8] and numerical results obtained for the magnetic induction component $B_x$ in the (*a*) $x$, (*b*) $y$, (*c*) $z$ directions, and (*d*) for the Lorentz force. Uncertainty of the magnetic induction measurements is 0.5 mT. Uncertainty of the Lorentz force measurements is 0.05 N.

results to the experimental value of $B_x$ in the center of the magnet system. The electrical conductivity of the Al bar is $\sigma = 22 \cdot 10^6\,\Omega^{-1}\mathrm{m}^{-1}$.

The numerically computed Lorentz forces at different heights of the aluminum bar (2.5 cm, 5 cm, 8 cm and 10 cm) and velocity $v = 5$ cm/s are also in a very good agreement with the experimental results (see Fig. 3*d*).

Therefore, the numerical computations for a moving solid conductor at a constant velocity show a very good agreement with the experimental measurements. But in practice we deal with turbulent or laminar flows in pipes or open channels. Computations of the Lorentz force, acting on the liquid metals flowing in a circular pipe, were performed in [10]. The results differ by only 2–3% when the turbulent flow computations at high Reynolds numbers ($\mathrm{Re} = 10^5 - 10^6$) are included into the discussed model. Therefore, the optimization of the LFF geometry will be performed for a solid conductor, which is moving at a constant velocity.

*2.2. Optimization of the flowmeter geometry.* a) Optimization of the magnet system geometry. The measurements performed by flowmeters tested in industrial applications have shown small values of the force, acting on the magnet system [3]. The efficiency of these flowmeters depends on the ratio between the Lorentz force and the mass of the magnet system

$$E = \frac{F}{M}. \tag{14}$$

Therefore, a numerical optimization of the flowmeter geometry in order to obtain a maximum Lorentz force at a minimum mass of the magnet is necessary.

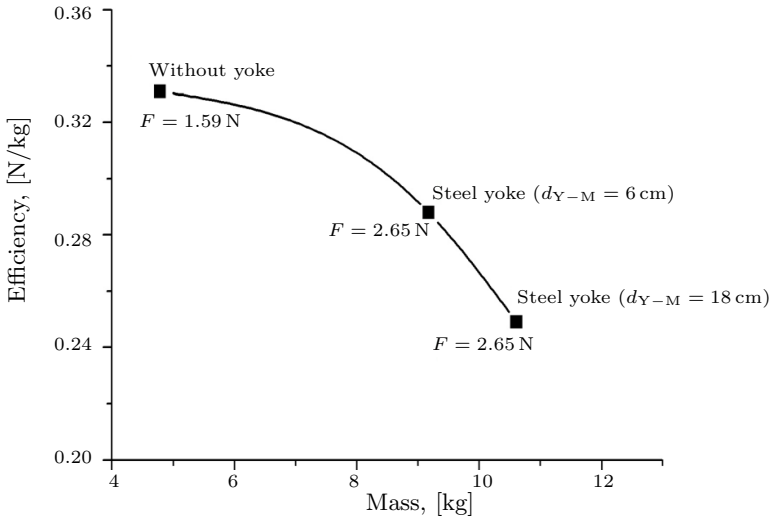


*Fig. 4.* Efficiency versus magnet system mass for configurations with and without a yoke.

Computations are performed for a solid conductor with the electrical conductivity $\sigma = 22 \cdot 10^6\,\Omega^{-1}\mathrm{m}^{-1}$, which is moving at the constant velocity $v = 5\,\mathrm{cm/s}$ trough the magnet system.

The first set of simulations investigates the influence of a steel yoke on the flowmeter efficiency. The simulations show a decreasing efficiency of the magnet systems with a Π-shape steel yoke (see Fig. 4). By increasing the distance between the magnet and the upper part of the yoke ($d_{\mathrm{Y-M}}$), the computed force is unchanged, but the flowmeter efficiency decreases because the magnet system becomes heavier.

Therefore, in the following, the optimization is performed for a magnet system without a yoke. The dimensions in the $x$, $y$ and $z$ directions for the magnets and the conductor are, respectively, $x_{\mathrm{M}}$, $y_{\mathrm{M}}$, $z_{\mathrm{M}}$ and $x_{\mathrm{C}}$, $y_{\mathrm{C}}$, $z_{\mathrm{C}}$ (see Fig. 2).

For the given configuration, the dimensions of the channel (moving conductor) and the distance between the magnets ($d$) are known, so the optimization is performed only for the magnet dimensions. Because the eddy currents, which contribute to the measurable Lorentz force ($F_y$), have the $z$ direction, the magnetic induction should be intense over the conductor cross-section area along the $z$-axis. Therefore, the magnet $z_{\mathrm{M}}$ dimension must be almost the same as that of the conductor $z_{\mathrm{C}}$. For open channel flows, the $z_{\mathrm{C}}$ dimension corresponds to the liquid metal level in the channel, which generally fluctuates during the casting process. In this case, the optimal $z_{\mathrm{M}}$ dimension must be the typical level of the liquid metal in the channel. The computations performed for different $z_{\mathrm{M}}$ dimensions show a maximum efficiency for $z_{\mathrm{M}} = 0.9 \cdot z_{\mathrm{C}}$ (see Fig. 5).

The results obtained from the optimizations of the $y_{\mathrm{M}}$ dimension are plotted in Fig. 6. The computations performed at different distances between the magnets ($d = 10, 20$ and $30\,\mathrm{cm}$) show that the optimal $y_{\mathrm{M}}$ dimension depends on the distance $d$. The optimal ratio $y_{\mathrm{M}}/d$ varies from 0.2 at $d = 30\,\mathrm{cm}$ to 0.6 at $d = 10\,\mathrm{cm}$.

In Fig. 7, the efficiency is plotted versus the magnet mass for two sets of simulations performed by increasing, respectively, the $x_{\mathrm{M}}$ and $y_{\mathrm{M}}$ dimension. Because in our configurations the magnet poles consist by arrangement of small NdFeB blocks, the $x_{\mathrm{M}}$ dimension can be increased only by 2 or 3 cm. The computations performed by increasing the $x_{\mathrm{M}}$ dimension have shown only a moderate increase

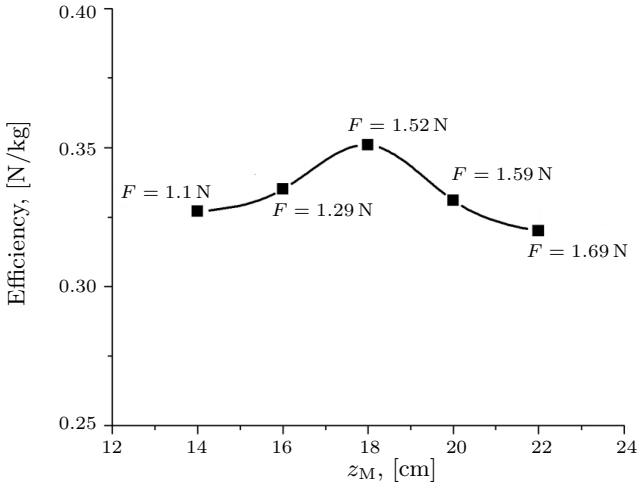


*Fig. 5.* Efficiency versus $z_M$ dimension of the magnets. ($x_M = 2$ cm, $y_M = 8$ cm, $x_C = 5$ cm, $z_C = 20$ cm, $d = 15$ cm).

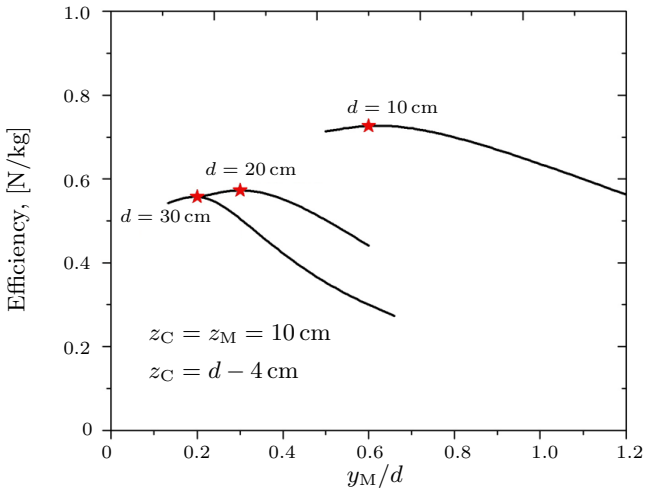


*Fig. 6.* Efficiency versus $y_M/d$ ratio for $d = 10, 20$ and 30 cm.

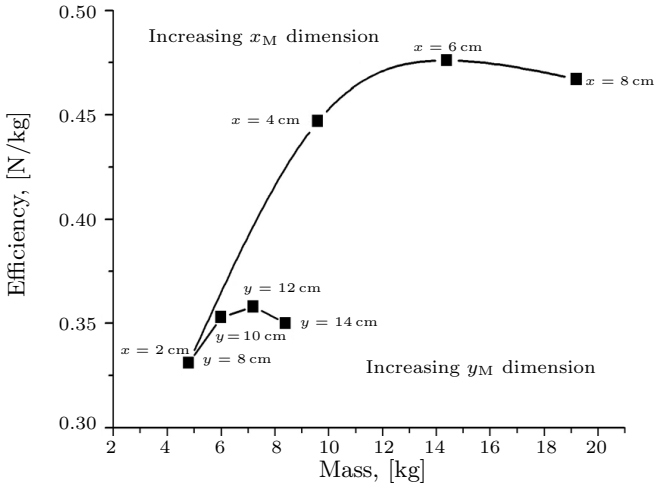


*Fig. 7.* Efficiency versus the magnet mass when, respectively, the $x_M$ and $y_M$ dimensions are increased. ($z_M = 20$ cm, $x_C = 5$ cm, $z_C = 20$ cm, $d = 15$ cm).

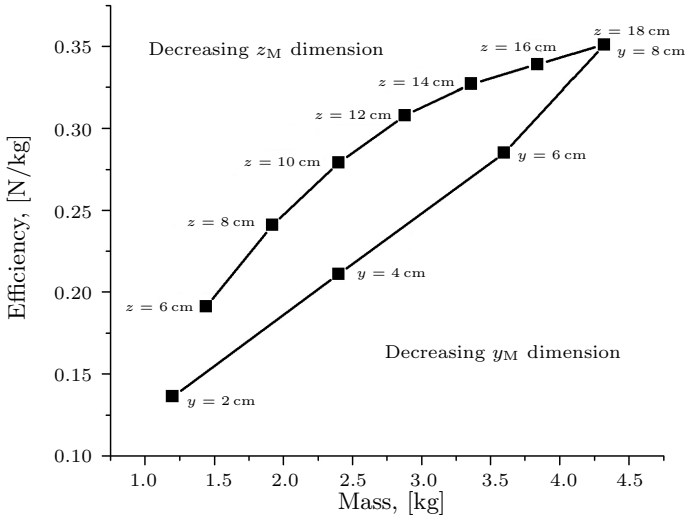


*Fig. 8.* Efficiency versus the magnet mass when, respectively, the $y_M$ and $z_M$ dimensions are decreased. ($x_M = 2\,\text{cm}$, $x_C = 5\,\text{cm}$, $z_C = 20\,\text{cm}$, $d = 15\,\text{cm}$).

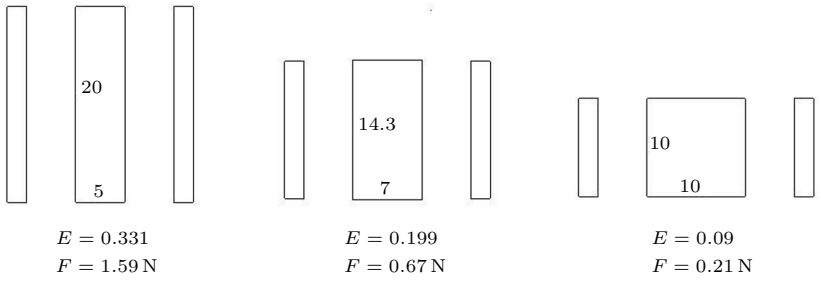


*Fig. 9.* Efficiency and Lorentz force computed at various aspect ratios of the conductor: $x_C/z_C = 0.25, 0.49, 1.0$. The conductor dimensions are given in centimeters. The distance between the channel and the magnets is kept constant at 5 cm.

of the efficiency at a significant increase of the magnet mass. In conclusion, the optimal $x_M$ dimension should be set at the minimum magnet block dimension (2 cm or 3 cm) and the efficiency can be increased by increasing the $y_M$ dimension.

This kind of optimizations can set the magnet dimensions in order to have a maximum efficiency of the flowmeter. The maximum efficiency is generally reached at a high mass of the magnet system. Sometimes, in practice, it is more useful to have a soft magnet system, which allows for a good sensitivity of the Lorentz force measurements. The simulations performed by decreasing, respectively, the $y_M$ and $z_M$ dimensions show that the sensitivity decreases more rapidly when $y_M$ is reduced (see Fig. 8). These results show that soft magnet systems of 2–3 kg can be used in practice for efficient measurements of the Lorentz force.

b) Optimization of the conductor geometry. The simulations performed for a conductor having a rectangular cross-section area of $S = 100\,\text{cm}^2$ and various aspect ratios $x_C/z_C$ (0.25, 0.49 and 1.0) show a significant reduction of the efficiency when the aspect ratio increases (see Fig. 9). The optimal shape of the conductor is given by $x_C/z_C = 0.25$, because, in this case, the distance between the magnets decreases ($d = 15\,\text{cm}$) and the conductor is in a region characterized by a high intensity of the magnetic field.

**3. Conclusions.** The COMSOL Multiphysics software is used for the optimization of the LFF geometry in order to improve the efficiency of Lorentz force measurements. The numerical model is validated by comparing the numerical results to the experimental data obtained from dry calibration experiments.

The optimization of rectangular channel dimensions shows an increasing Lorentz force when the aspect ratio of channels decreases. The magnet system efficiency is improved when the magnet dimensions are augmented in the flow direction, because, in this case, the electrically conducting volume exposed to a magnetic field increases. Soft magnet configurations without a yoke, weighting 2–3 kg, can be used also in practice. For industrial applications, where the channel's width is large and the liquid metals have low electrical conductivities or flow at low velocities, the magnet mass must be increased in order to provide a measurable Lorentz force. Generally, it is difficult to set an algorithm for the optimization procedure. The optimal geometry of this device depends on particular conditions given for each configuration: channel shape, mean flow velocity, electrical conductivity of metal, sensitivity of the force sensor, etc.

**Acknowledgments.** The authors are grateful to the German Research Foundation (Deutsche Forschungsgemeinschaft) for supporting the work in the frame of the Research Training Group (Graduiertenkolleg) Lorentz force velocimetry and Lorentz force eddy current testing at Ilmenau University of Technology. We are grateful to Bundesministerium für Bildung and Forschung for financial support in the framework of the ForMaT program. The authors also acknowledge stimulating discussions with M. Gramss, M. Kirpo, V. Minchenya, X. Wang, R. Klein and A. Thieme.

## REFERENCES

[1] J. Shercliff. *The Theory of Electromagnetic Flow Measurements* (Cambridge University Press, Cambridge, UK, 1962).

[2] A. Thess, E.V. Votyakov, and Y. Kolesnikov. Lorentz force velocimetry. *Phys. Rev. Lett.*, vol. 96 (2006), p. 164501.

[3] A. Thess, E.V. Votyakov, B. Knaepen, and O. Zikanov. Theory of the Lorentz force flowmeter. *New J. Phys.*, vol. 9 (2007), p. 299.

[4] Y. Kolesnikov, C. Karcher, and A. Thess. Lorentz force flowmeter for liquid aluminium: Laboratory experiments and plant tests. *Metall. Mater. Trans. B*, vol. 42 (2011), no. 3, p. 441.

[5] M. Kirpo, S. Tympel, T. Boeck, D. Krasnov, and A. Thess. Electromagnetic drag on a magnetic dipole near a translating conducting bar. *J. Appl. Phys.*, vol. 109 (2011), p. 113921.

[6] R. Ricou and C. Vives. Local velocity and mass transfer measurements in molten metals using incorporated magnet probe. *Int. J. Heat Mass Tran.*, vol. 25 (1982), pp. 1579–1588.

[7] V. Minchenya, C. Karcher, Yu. Kolesnikov, and A. Thess. Dry calibration of the Lorentz force flowmeter. *Magnetohydrodynamics*, vol. 45 (2009), no. 4, pp. 569–578.

[8] V. Minchenya. *Lorentz force flowmeter for open channels. Results of the dry calibration experiments 2007-2008* (Report Ilmenau University of Technology, 2009).

[9] M. Gramss, R. Klein, A. Thess. *Development of a Lorentz force flowmeter to measure flow rates in aluminum melts* (13-th MHD Days, November, 2010, Dresden).

[10] C. Stelian, A. Alferenok, U. Luedtke, Y. Kolesnikov, and A. Thess. *Numerical optimization and calibration of a Lorentz force flowmeter.* (submitted to the 8th PAMIR International Conference on Fundamental and Applied MHD, Borgo-Corsica, France, September 5-9, 2011).

Received 11.08.2011